

Behavior of circular thin-walled steel tube confined concrete stub columns

Fa-xing Ding¹, Liu Tan¹, Xue-mei Liu² and Liping Wang^{*1}

¹ School of Civil Engineering, Central South University, Changsha, Hunan Province, 410075, P.R. China

² School of Civil Engineering and Built Environment, Queensland University of Technology, Brisbane, QLD 4000, Australia

(Received July 26, 2016, Revised December 04, 2016, Accepted December 23, 2016)

Abstract. This paper presents a combined numerical and theoretical study on the composite action between steel and concrete of circular steel tube confined concrete (STCC) stub columns under axial compressive loading with a full theoretical elasto-plastic model and finite element (FE) model in comparison with experimental results. Based on continuum mechanics, the elasto-plastic model for STCC stub columns was established and the analysis was realized by a FORTRAN program and the three dimensional FE model was developed using ABAQUS. The steel ratio of the circular STCC columns were defined in range of 0.5% to 2% to analyze the composite action between steel tube and concrete, and make a further study on the advantages of the circular STCC columns. By comparing the results using the elasto-plastic methods with the parametric analysis result of FE model, the appropriate friction coefficient between the steel tube and core concrete was defined as 0.4 to 0.6. Based on ultimate balance theory, the formula of ultimate load capacity applying to the circular STCC stub columns was developed.

Keywords: circular steel tube; confinement; composite action; stress-strain relationship; elasto-plastic methods; ABAQUS

1. Introduction

In recent years, concrete-filled steel tube (CFT) columns have been widely used as structural members, and numerous studies on circular CFT columns have been conducted (Schneider *et al.* 1998, Aboutaha and Machado 1998, Chang *et al.* 2009, Huang *et al.* 2008, 2012, Lee *et al.* 2011, Wang and Chang 2013, Ren *et al.* 2014, Kim *et al.* 2015, Cui and Shao 2015). Aimed at improving the poor seismic performance of the CFT stub columns, Tomii *et al.* (1987) firstly proposed the concept of circular STCC stub column in 1985, in which the axial loading was undertaken only by the core concrete while the steel tube was used only for lateral confinement. Tomii *et al.* (1987) replaced the stirrup in reinforced concrete columns with steel tube, and the steel tube did not bear vertical load directly. Later, O'shea and Bridge (2000) presented the experimental investigation and theoretical analysis on the mechanical behavior of concrete filled circular thin-walled steel stub column with steel ratio between 1.5-6% under different loading conditions. Besides, O'shea and Bridge (2000) developed three design methods to conservatively estimate the strength of concrete filled circular thin-walled steel tubes under axial loading of the steel only, axial loading of the concrete only, and simultaneous loading of the concrete and steel, respectively. The results showed that the confinement effect of the steel tube on the core concrete existed from the beginning of loading for circular STCC

stub columns, and the ultimate capacity of the STCC stub columns was higher than that of the CFT stub columns. Johansson and Gylltoft (2002) established 3D finite element models using ABAQUS to analyze the circular STCC stub columns at the steel ratio of 11.7%, revealed the variations of the internal forces during the loading process, and investigated the mechanic behavior of the circular STCC stub columns. Han *et al.* (2005) studied the monotonic and cyclic behavior of STCC columns with square and circular sectional shapes, it was found that the capacity and ductility of STCC columns is higher than that of CFT columns for both two shapes. Based on the study by Han *et al.* (2005), Qing *et al.* (2010) proposed a formula to calculate the ultimate load capacity of the STCC stub columns under axial load. To take full advantages of circular STCC columns, Liu *et al.* (2009) presented the experimental investigation on the mechanical behavior of circular tube confined reinforced-concrete (CTRC) with steel ratio between 9-18%, showing that both the ultimate capacity and the ductility of the CTRC are improved significantly compared with CFT. In fact, the steel tube of the circular STCC column basically plays the role of stirrup, which only provides confinement effect on the concrete rather than directly bearing the load. Moreover, it is found that the axial stiffness of STCC column is lower than CFT counterparts when the steel ratio is larger than 2%.

Therefore, this study aims at investigating the behavior of circular STCC columns with lower steel ratios ranging from 0.5% to 2%. On the basis of previous research (Yu *et al.* 2007, Ding *et al.* 2011a, 2014, 2015), several issues were further addressed in this study: (1) Investigated the mechanical performance of circular STCC stub columns under uniaxial loading using the elasto-plastic method and

*Corresponding author, Lecturer,
E-mail: wlp2016@csu.edu.cn; kachywlp@gmail.com

nonlinear FEA; (2) Analyzed the composite action between steel and concrete of the circular STCC stub columns with two different theoretical methods, and studied the influence of different friction coefficients between the steel tube and core concrete on the FEA results; (3) Established the design formula of ultimate load capacity for the circular STCC stub column.

2. Theoretical model

2.1 Elasto-plastic method

2.1.1 Basic assumption

- (1) The constitutive relationship of concrete and the strength criterion proposed in Ding *et al.* (2011a) was adopted for the current study.

$$y = \begin{cases} \frac{A_2 x + (B_2 - 1)x^2}{1 + (A_2 - 2)x + B_2 x^2} & x \leq 1 \\ \frac{x}{\alpha_2 (\lambda - 1)^2 + x} & x > 1 \end{cases} \quad (1)$$

where $y = \sigma_{L,c}/f_{cc}$; $x = \varepsilon_{L,c}/\varepsilon_{cc}$; $\sigma_{L,c}$ is the axial stress of concrete subjected to lateral confining pressure; $\varepsilon_{L,c}$ is the axial strain of concrete subjected to lateral confining pressure; f_{cc} is the axial compressive strength of concrete subjected to lateral confining pressure; ε_f is the peak axial strain of concrete; $f_c = 0.4f_{cu}^{7/6}$; $\varepsilon_c = 383 f_{cu}^{7/18} \times 10^{-6}$; $A_1 = 9.1 f_{cu}^{-4/9}$; $B_1 = 1.6(A_1 - 1)^2$; $f_{cc}/f_c = 1 + 3.4\sigma_{r,c}/f_c$; $\varepsilon_f = \varepsilon_c(1 + 3.4\sigma_{r,c}/f_c)[1 + 4.8(A_1 - 1)(\sigma_{r,c}/f_c)^{0.5}]$; $A_2 = A_1[1 + 4.8(A_1 - 1)(\sigma_{r,c}/f_c)^{0.5}]$; $B_2 = \frac{y + (A_2 - 2)xy - (A_2 - x)x}{(1 - y)x^2}$; and α_2

$= 0.15$ is the decline coefficient for the descending branch of the axial stress–strain relationship. The definition of other parameters can refer to Ding *et al.* (2011a).

- (2) The constitutive model for steel and the strength criterion proposed in Ding *et al.* (2011a) was adopted for the current study.

$$\sigma_i = \begin{cases} E_s \varepsilon_i & \varepsilon_i \leq \varepsilon_y \\ f_s & \varepsilon_y < \varepsilon_i \leq \varepsilon_{st} \\ f_s + \zeta E_s (\varepsilon_i - \varepsilon_{st}) & \varepsilon_{st} < \varepsilon_i \leq \varepsilon_u \\ f_u & \varepsilon_i > \varepsilon_u \end{cases} \quad (2)$$

where σ_i is the equivalent stress of steel; f_s is the yield strength; f_u is the ultimate strength, $f_u = 1.5f_s$; E_s is the elastic modulus, $E_s = 206,000$ MPa; E_{st} is the strengthening modulus, which is described by $E_{st} = \zeta E_s$; ε_u is the ultimate strain, which is described by $\varepsilon_u = \varepsilon_{st} + 0.5f_s/(\zeta E_s)$; ζ and ε_{st} are coefficients. In this paper, it was considered that $\varepsilon_{st} = 12\varepsilon_y$ and $\varepsilon_u = 120\varepsilon_y$, and the resulting value of ζ is 1/216

- (3) Deformation coordination assumptions: The steel tube and concrete co-worked well with deformation compatibility and interface continuity.

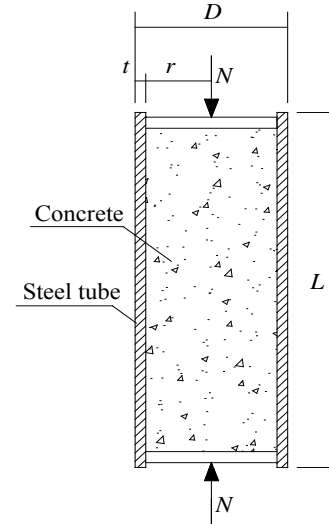


Fig. 1 Calculation model of STCC

2.1.2 Formulation in elastic stage

The concentric concrete cylinder of the STCC stub column can be analyzed through the computing model as shown in Fig. 1.

In the conditions of small deformation, the STCC stub column remains as an axisymmetric generalized plane strain problem under the scope of elastic mechanics. Introducing Airy stress function herein

$$\Gamma = C_1 \ln r + C_2 r^2 \ln r + C_3 r^2 + C_4 \quad (3)$$

where C_1 , C_2 , C_3 and C_4 are undetermined coefficients, r is the radius of the cylinder. Then we can obtain the general form of elastic solution

- (a) For concrete core section [$0 < r \leq (D/2 - t)$]

Stress

$$\sigma_{r,c} = \sigma_{\theta,c} = 2C_3 \quad (4)$$

$$\sigma_{L,c} = E_c \varepsilon_{L,c} + 4\nu_c C_3 \quad (5)$$

$$u_{L,c} = L \varepsilon_{L,c} \quad (6)$$

Strain

$$\varepsilon_{r,c} = \varepsilon_{\theta,c} = 2C_3(1 - \nu_c - 2\nu_c^2)/E_c - \nu_c \varepsilon_{L,c} \quad (7)$$

Displacement

$$u_{r,c} = r[2C_3(1 - \nu_c - 2\nu_c^2)/E_c - \nu_c \varepsilon_{L,c}] \quad (8)$$

- (b) For steel tube section [$(D/2 - t) \leq r \leq D/2$]

Stress

$$\sigma_{r,s} = A/r^2 + 2B \quad (9)$$

$$\sigma_{\theta,s} = -A/r^2 + 2B \quad (10)$$

$$\sigma_{L,s} = E_s \varepsilon_{L,s} + 4\nu_s B = 0 \quad (11)$$

Strain

$$\begin{cases} \varepsilon_{r,s} = \frac{1+\nu_s}{E_s} \frac{A}{r^2} + \frac{2B(1-\nu_s-\nu_s^2)}{E_s} - \nu_s \varepsilon_{L,s} \\ \varepsilon_{\theta,s} = -\frac{1+\nu_s}{E_s} \frac{A}{r^2} + \frac{2B(1-\nu_s-\nu_s^2)}{E_s} - \nu_s \varepsilon_{L,s} \end{cases} \quad (12)$$

Displacement

$$\begin{cases} u_{r,s} = r \left[\frac{2B(1-\nu_s-\nu_s^2)}{E_s} - \nu_s \varepsilon_{L,s} \right] - \frac{1+\nu_s}{E_s} \frac{A}{r} \\ u_{L,s} = L \varepsilon_{L,s} \end{cases} \quad (13)$$

In Eqs. (4)-(13), $\sigma_{L,c}$ and $\sigma_{L,s}$ are the axial stress of concrete and steel respectively; $\sigma_{r,s}$ and $\sigma_{\theta,s}$ are the radial and hoop stress of steel respectively; $\varepsilon_{L,c}$ and $\varepsilon_{L,s}$ are the axial strain of concrete and steel respectively; $\varepsilon_{r,c}$ and $\varepsilon_{\theta,c}$ are the radial and hoop strain of concrete respectively; $\varepsilon_{r,s}$ and $\varepsilon_{\theta,s}$ are the radial and hoop strain of steel respectively; ν_s and ν_c are the poisson's ratio of concrete and steel respectively; E_s and E_c are the modulus of elasticity of concrete and steel respectively; $u_{r,c}$ and $u_{L,c}$ are the radial and axial displacement of concrete respectively; $u_{r,s}$ and $u_{L,s}$ are the radial and axial displacement of steel respectively; A and B are undetermined constants; L is the length of the cylinder; D is the diameter of the cylinder; t is the thickness of the cylinder.

For the circular STCC, the axial compression load is undertaken by concrete, and

$$\sigma_{L,c} A_c = N \quad (14)$$

where, A_c is the area of concrete, N is the external load.

Based on the continuum mechanics, the undetermined constants A , B and C_3 can be determined with the boundary conditions of stress and interface continuity conditions of the STCC columns:

(1) For concrete core section [$0 < r \leq (D/2 - t)$]

Stress

$$\sigma_{r,c} = \sigma_{\theta,c} = \rho \nu_c Q' \cdot E_s \varepsilon_{L,c} \quad (15)$$

$$\sigma_{L,c} = E_c \varepsilon_{L,c} + 2\rho \nu_c^2 Q' E_s \varepsilon_{L,c} \quad (16)$$

Strain

$$\varepsilon_{r,c} = \varepsilon_{\theta,c} = \rho \nu_c (1 - \nu_c - 2\nu_c^2) Q' n \varepsilon_{L,c} - \nu_c \varepsilon_{L,s} \quad (17)$$

(2) For steel tube section [$(D/2 - t) \leq r \leq D/2$]

Stress

$$\begin{cases} \sigma_{r,s} = [(D/2r)^2 - 1](1 - \rho) \nu_c Q' \cdot E_s \varepsilon_{L,c} \\ \sigma_{\theta,s} = -[(D/2r)^2 + 1](1 - \rho) \nu_c Q' \cdot E_s \varepsilon_{L,c} \\ \sigma_{L,s} = 0 \end{cases} \quad (18)$$

Strain

$$\begin{cases} \varepsilon_{r,s} = [(D/2r)^2 (1 + \nu_s) - (1 - \nu_s - \nu_s^2) + 2\nu_s^2](1 - \rho) \nu_c Q' \varepsilon_{L,c} \\ \varepsilon_{\theta,s} = -[(D/2r)^2 (1 + \nu_s) + (1 - \nu_s - \nu_s^2) - 2\nu_s^2](1 - \rho) \nu_c Q' \varepsilon_{L,c} \\ \varepsilon_{L,s} = 2(1 - \rho) \nu_s \nu_c Q' \varepsilon_{L,c} \end{cases} \quad (19)$$

where $Q' = [(1 - \nu_c - 2\nu_c^2)n\rho + (2 + \nu_s^2 - \rho + \rho\nu_s - \rho\nu_s^2)]^{-1}$, $n = E_s/E_c$, $\rho = A_s/A_{sc}$, $A_{sc} = A_s + A_c$, A_s is the area of steel.

Substituting the expressions of $\sigma_{L,c}$ in Eqs. (15)-(16) to Eq. (14), the composite stress-strain relationship of the stub column in elastic stage can be written as

$$f_{sc} = \sigma_{L,c} = E_{sc} \varepsilon_{L,c} \quad (20)$$

$$E_{sc} = E_c + 2\rho \nu_c^2 Q' E_s \quad (21)$$

In Eq. (18), E_{sc} is the composite modulus of elasticity. Since the term $\rho \nu_c^2$ is infinitesimal, the composite modulus of elasticity of circular STCC stub column is barely larger than the uniaxial compression modulus of elasticity of core concrete and the steel tube doesn't play any role under compression.

2.1.3 Formulation in inelastic stage

The poisson's ratio of core concrete and the compression stress between the steel tube and core concrete are increasing as the load increases. The internal edge of the steel tube contacted with core concrete (where $r = D/2 - t$) would yield first. In fact, the inside and outside surface of the steel tube would yield almost at the same time due to the thin tube wall. The radial stress of steel tube was ignored in analyzing the stress of the steel tube in plastic stage. According to Eq. (18), the stresses of steel tube after yield can be written as

$$\begin{cases} \sigma_{\theta,s} = -2\nu_c (1 - \rho) Q'_t \cdot E_s^t \varepsilon_{L,c} \\ \sigma_{L,s} = 0 \end{cases} \quad (22)$$

where $Q'_t = [(1 - \nu_c - 2\nu_c^2)n_t\rho + (2 + \nu_s^2 - \rho + \rho\nu_s - \rho\nu_s^2)]^{-1}$, $n_t = E_s^t/E_c^t$, E_s^t and E_c^t are secant modulus of steel and concrete in inelastic stage respectively.

The strains at mid-height of steel tube after yield were expressed as

$$\begin{cases} \varepsilon_{r,s} = [(1 + \nu_s)/(1 - \rho/4) - (1 - \nu_s - \nu_s^2) + 2\nu_s^2](1 - \rho) \nu_c Q'_t \varepsilon_{L,c} \\ \varepsilon_{\theta,s} = -[(1 + \nu_s)/(1 - \rho/4) + (1 - \nu_s - \nu_s^2) - 2\nu_s^2](1 - \rho) \nu_c Q'_t \varepsilon_{L,c} \\ \varepsilon_{L,s} = 2(1 - \rho) \nu_s \nu_c Q'_t \varepsilon_{L,c} \end{cases} \quad (23)$$

The strains on the external surface of the steel tube after yield can be calculated by Eq. (18).

As a result, the composite stress-strain relationship of the circular STCC stub column in inelastic stage can be written as

$$f_{sc} = \sigma_{L,c} = E_{sc}^t \varepsilon_{L,c} \quad (24)$$

where $E_{sc}^t = E_c^t + 2\nu_c^2 \rho Q'_t E_s^t$.

2.2 FE models

FE models were created using ABAQUS/Standard 6.10 to compare the interactive behaviour between the steel and concrete for circular STCC stub columns and circular CFT stub columns, respectively. The core concrete and loading plates were defined as rigid bodies. A structured meshing option was adopted, and the mesh results are shown in Fig. 2. A surface-to-surface contact was adopted for the con-

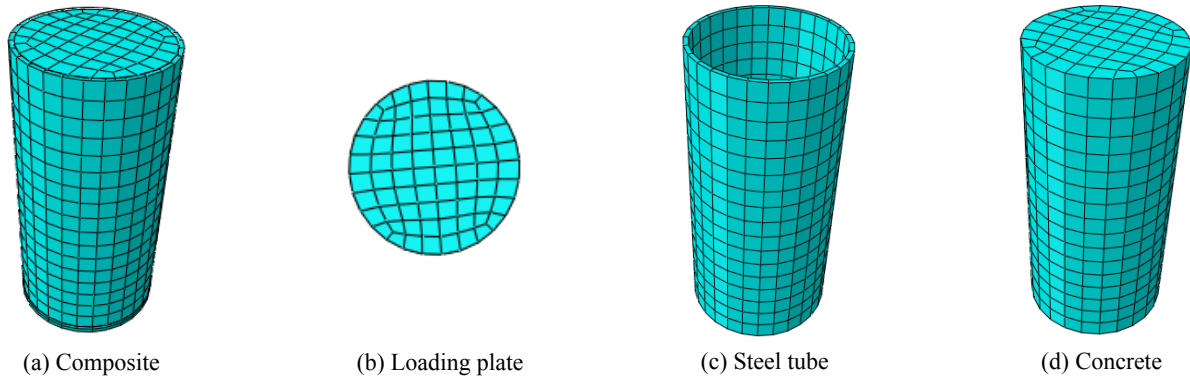


Fig. 2 Mesh generation of model

straint between the steel tube (master surface) and the concrete (slave surface). In the proposed FE model, the shear stress between the steel tube and core concrete is generated by friction and an appropriate friction coefficient (μ) of 0.5 was adopted, which was identical with the value used in prior research (Yu *et al.* 2007). The sliding formulation was finite sliding, and a hard contact was defined in the normal direction.

For the CFT stub columns, tie constraints was adopted for the core concrete and loading plate, and the steel tube and loading plate, respectively, which ensure that the core concrete and the steel tube can share the load together in the whole loading process. For the STCC stub columns, a tie constraint was adopted for the core concrete and loading plate which ensures that only the core concrete would take load. Rigid surface was used to simulate the loading plate, of which the modulus of elasticity was taken as 1.0×10^{11} , and the Poisson's ratio was assumed to be 1.0×10^{-7} .

The following non-dimensional mathematical form for the stress-strain relationship of concrete under uniaxial compression was proposed in Ding *et al.* (2011a, 2014)

$$y = \begin{cases} \frac{A_1 x + (B_1 - 1)x^2}{1 + (A_1 - 2)x + B_1 x^2} & x \leq 1 \\ \frac{x}{\alpha_1 (\lambda - 1)^2 + x} & x > 1 \end{cases} \quad (25)$$

In the FE models, the damage plasticity model of concrete defined in ABAQUS was used, and some parameters of concrete supposed by Ding *et al.* (2011a) are shown as follow: the eccentricity is 0.1; the ratio of initial equibiaxial compressive yield stress to initial uniaxial compressive yield stress is 1.225; the ratio of the second stress invariant on the tensile meridian to that on the compressive meridian is $2/3$; the viscosity parameter is 0.005; and the dilation angle is 40° . The value of dilation angle was obtained by comparing the ordinary concrete-filled steel tube column and concrete-filled steel tube columns with lightweight aggregate concrete (Ding *et al.* 2011b, c). The concrete model established by ABAQUS has considered the confined interaction of the steel tube on the core concrete with the above parameters, which was proved to be suitable for numerical analysis on triaxial-compressed concrete in STCC columns and CFT columns.

The constitutive model for steel and the strength criterion is given in Eq. (2). In order to obtain the descending branch of uniaxial stress-strain curve, displacement loading was used to simulate the whole loading process and the incremental iterative method was used for solving nonlinear formulas in the FEA.

3. Experimental verification and analysis

3.1 Experimental verification

The composite stress-strain relationship of circular STCC was obtained by using the elasto-plastic nonlinear analysis and non-linear FEA. 27 groups of test data from the studies by O'shea and Bridge (2000), Han *et al.* (2005) and Yu *et al.* (2007) were collected to verify the practicality of the above two methods. The average ratios of the test data over the theoretical and numerical results are shown in Table 2. It can be seen that the results obtained from FEA and the elasto-plastic methods are in good agreement with the test results. The typical comparison is shown in Fig. 3 for the load dependent strain development. Small differences of initial stiffness of specimens between the results from the tests and FE model were observed, which may be caused by the slippage between the concrete and reinforcement bars, and the small gaps between the test set up and specimens were ignored in the FE model to save the computation time.

The axial load (N) versus strain ratio (v_{sc}) curves of the circular STCC stub column and the circular CFT stub column were shown in Fig. 4. The strain ratio, proposed by Ding *et al.* (2016), which is defined as the absolute value of the hoop tensile strain divided by the axial strain, reveals the confinement effect of the core concrete offered by the steel tube. The higher the strain ratio is, the more the confinement effect is between the core concrete and steel tube. At the initial loading stage, the strain ratio of the circular STCC stub column is higher than that of the circular CFT stub column, which indicates the former steel tube made more contribution to bearing the transverse tensile force. The strain ratio of the circular CFT stub column reached the Poisson's ratio of steel when the load reached about 75% of the ultimate capacity. However, the strain ratio of the circular STCC stub column reached the Poisson's ratio of steel when the load reached about 90% of

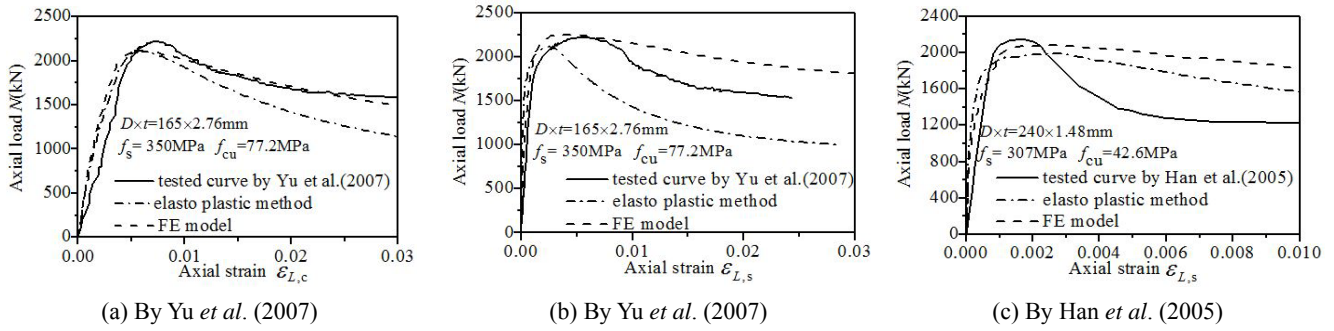


Fig. 3 Comparison of load-strain relations between calculated and test curves

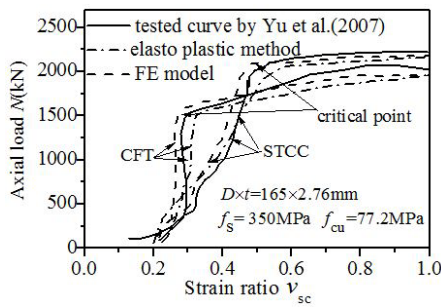


Fig. 4 Comparison of load-transverse strain curves obtained from tests and calculation

the ultimate capacity. Overall, it is demonstrated that the steel tube of circular STCC stub column has better confinement effect on the core concrete than that of circular CFT stub column.

3.2 Parametric analysis and discussion

According to the analysis from the elasto-plastic methods and the validated FE models of the circular STCC stub columns, the composite stress-strain relationships of the circular STCC and CFT stub columns considering different steel ratios, concrete strength and steel strength are shown in Fig. 5. The composite action between steel and concrete of the internal force is shown in Fig. 7. Different friction coefficients (μ) defined as 0 to 0.6 in FE models were adopted and the results were compared with that using the elasto-plastic methods. In general, the results obtained from the FE models are in good agreement with results using elasto-plastic methods when the friction coefficient is

0.4 to 0.6, as shown in Fig. 8.

When the core concrete is in elastic stage, the confinement effect of steel tube on the concrete is very small. Since the steel tube does not undertake the axial stress, the composite modulus of elasticity of the circular STCC is smaller than the circular CFT. Based on the analysis of internal force in the elastic stage, the steel tube is in the state of hoop tension with small confinement effect on the concrete at the beginning. The core concrete is under three-dimensional pressure under loading, of which the axial stiffness is consistent with the stiffness of concrete. Compared to the circular CFT, the elastic stage of circular STCC is longer, as shown in Fig. 5.

Under the load condition of axial pressure, the confinement effect is increasing with the increased poisson's ratio of the core concrete and the hoop tensile stress of the steel tube. After the yielding of the steel tube, the STCC enters the elasto-plastic stage, and its elasto-plastic stage is shorter than that of the circular CFT. The hoop tensile stress of the steel tube is essentially unchanged after yielding according to the internal force analysis at elasto-plastic stage, which indicates that the confinement effect is maximized. Because the confinement effect of steel tube in STCC is larger than that in CFT, the axial stress of STCC would be larger. As shown in Figs. 6 and 7, the ultimate capacity of the circular CFT stub columns (N_u (STCC)) is basically as same as the ultimate capacity of the circular STCC stub columns (N_u (CFT)). However, for the circular STCC stub columns, the radial stress of concrete ($\sigma_{r,c}$) is about 70% higher than that of the circular CFT stub columns, and the hoop stress of steel ($\sigma_{\theta,s}$) is about 30% higher than that of CFT stub columns. The circular STCC stub column has more practical advantages compared to the

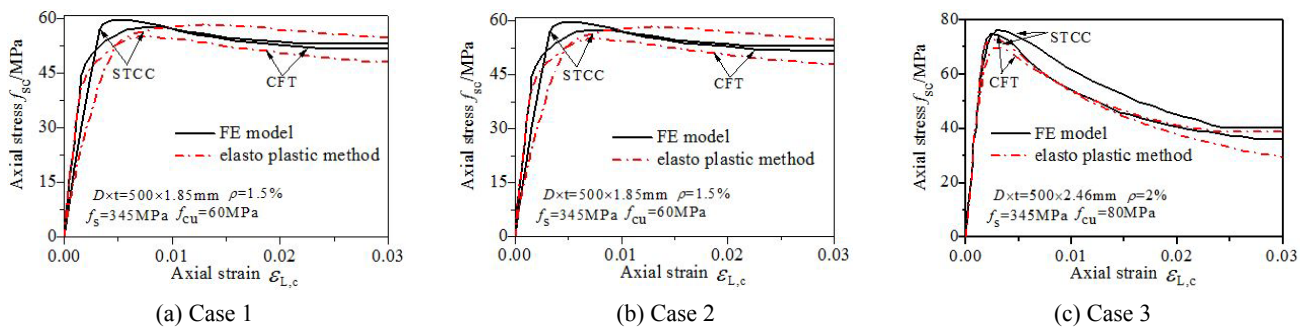


Fig. 5 Comparison of the composite stress-strain relations between CFT and STCC stub columns

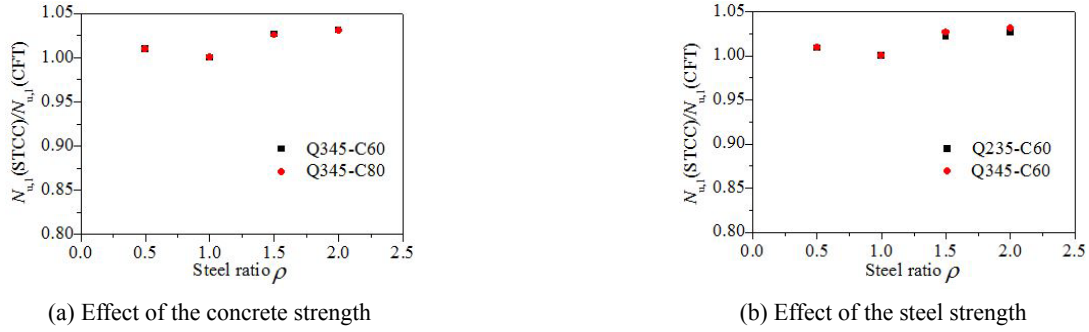


Fig. 6 Relationship between ultimate capacity ratio of STCC to CFT and steel ratio

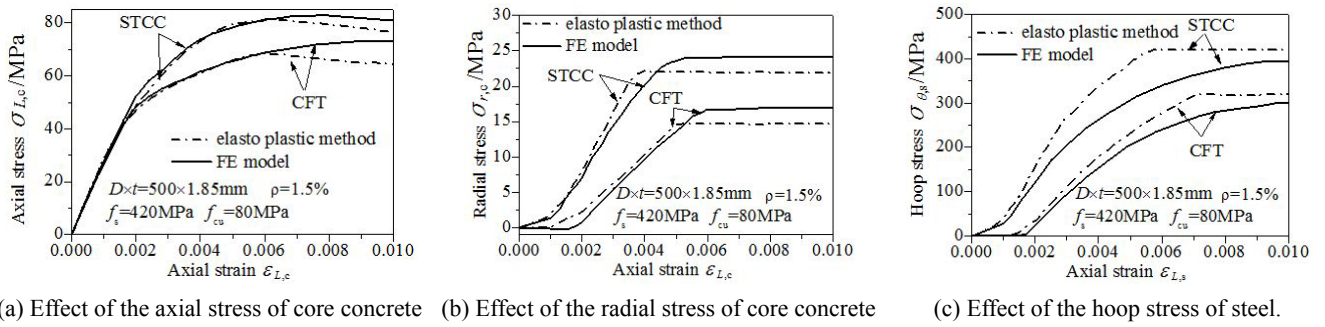


Fig. 7 Comparison of the stress-strain relations between CFT and STCC stub columns

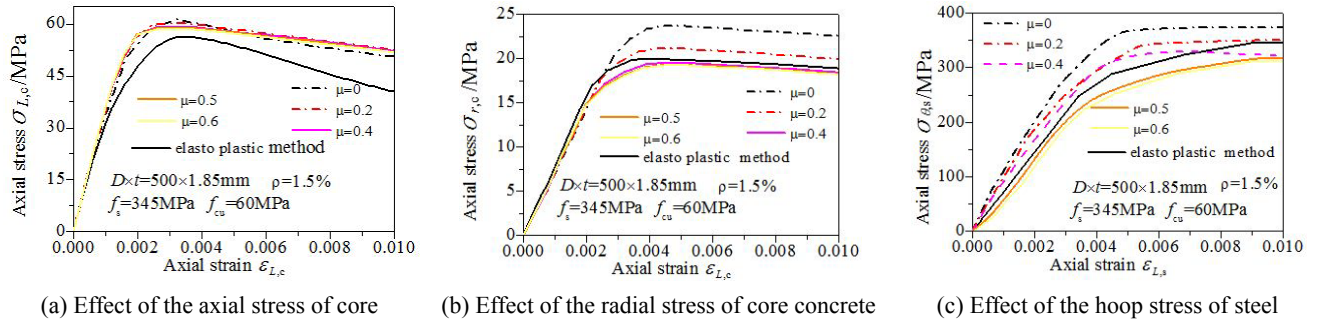


Fig. 8 Comparison of the stress-strain relations between elasto-plastic model and the FE model

circular CFT stub column regarding to the higher load bearing capacity, better ductility and remarkable composite action. Therefore, the circular STCC stub columns are widely adopted in engineering applications in China (Zhou and Liu 2010).

The circular STCC stub columns reaches its ultimate load capacity at the same time when the core concrete reaches its limit state, and the load capacity of the circular STCC stub columns is slightly higher than the circular CFT stub columns. The results of elasto-plastic analysis show that the circular STCC stub columns have better performance and higher residual load bearing capacity, while the results from FEA show little differences between them at the ultimate stage. The internal force analysis shows that the hoop tensile stress of steel tube is in the stage of yield or fortified at the ultimate stage, and the axial stress of core concrete of circular STCC stub columns is higher than that of the CFT stub columns. The comparison of the failure stress contours between the circular STCC and the circular CFT stub columns is presented in Fig. 9. It is shown that the

pressure stress in the middle section of concrete and the Mises yield stress of steel tube of the circular STCC stub columns are higher and more uniform than those of the circular CFT stub columns at the ultimate stage.

4. Formula for the ultimate load capacity

4.1 Formula establishment

For circular STCC stub columns, when the core concrete is in the ultimate state, supposing that the steel tube is at its perfectly plastic state and conform to the theory of continuum mechanics, the linear expression of the strength criterion for concrete core is given as

$$\sigma_{r,c} = \frac{\rho}{2(1-\rho)} f_s \quad (26)$$

According to Eq. (14), the following formula can be obtained

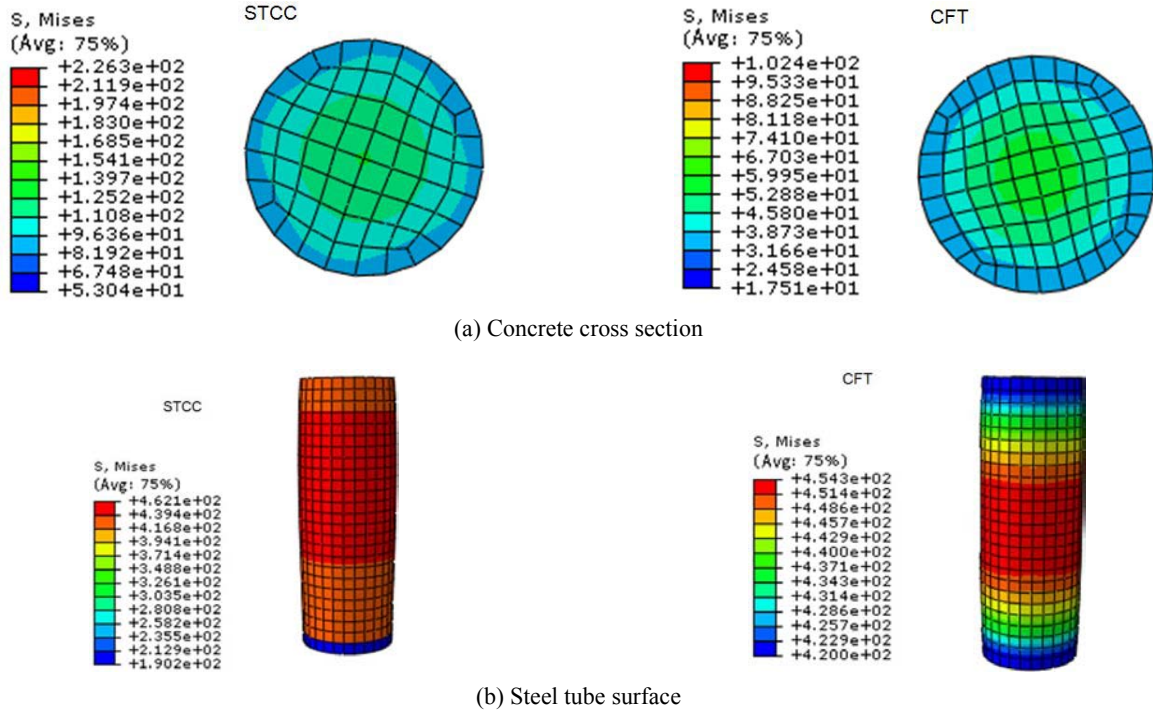


Fig. 9 Comparison of failure stress contours between the CFST and STCC stub columns

$$N_u = f_c^* A_c = (1 + 3.4\sigma_{r,c}/f_c) f_c A_c \quad (27)$$

Substituting the expression of $\sigma_{r,c}$ in Eq. (26) to Eq. (27), the ultimate load capacity of circular STCC stub column can be expressed as

$$N_u = (1 + 1.7\phi) f_c A_c \quad (28)$$

where ϕ is the confinement index, $\phi = A_s f_s / (A_c f_c)$.

Based on the elasto-plastic methods and FE models, the influence of parameters such as the concrete strength (f_{cu}), steel ratio (ρ , area ratio of steel tube to concrete) and yield strength of steel (f_s) on the ultimate load capacity of circular STCC stub column and the circular CFT stub column, respectively, were extensively investigated. A total of 18 FE models were established. The parameters used for the parametric study were detailed as below. (1) The external diameter of the cross section of the circular STCC column and the circular CFT column were 500 mm, the length was 1500 mm, and wall thickness of the steel tube were set as

0.60, 1.24, 1.85 and 2.46 mm, resulting the steel ratio of 0.5%, 1.0%, 1.5% and 2%, respectively; (2) The selected compressive strength of concrete was 40, 60, 80 and 100 MPa, the yield strengths of steel at 235, 345, and 420 MPa were used. (3) The following steel and concrete were paired for the columns: Q235 steel with C40 and C60 concrete, Q345 steel with C60 and C80 concrete, Q420 steel with C80 and C100 concrete.

Fig. 9 shows the comparison between the calculated ultimate capacities from the FE models ($N_{u,1}$) and the predicted ultimate capacities using the simplified formula determined by Eq. (28) ($N_{u,3}$). The calculated ultimate capacities by the elasto-plastic methods ($N_{u,2}$) and the predicted ultimate capacities using the simplified formula were also compared in Fig. 10. The average values and dispersion coefficient for various cases are shown in Table 1. It is indicated that the proposed formula is in a good agreement with the FE results and the elasto-plastic methods, and both FE modeling and the elasto-plastic

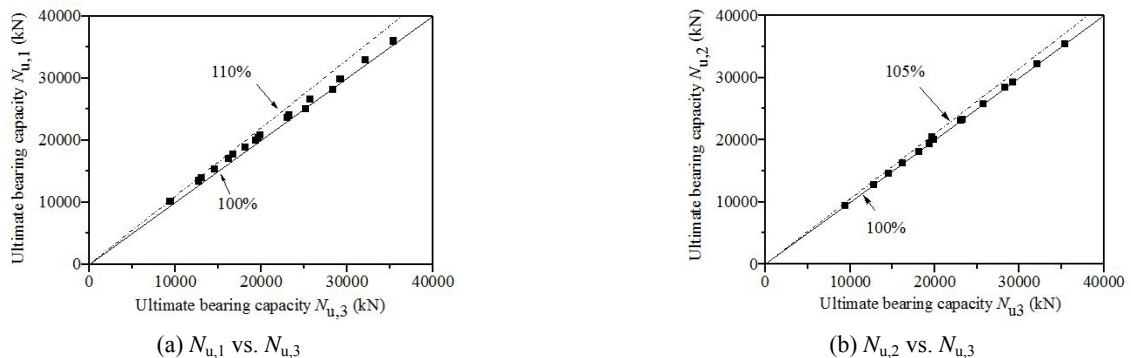


Fig. 10 Comparison of the bearing capacity obtained from FE models, elasto-plastic methods and Eq. (28)

Table 1 Average values and dispersion coefficient for various cases

	$N_{u,1}/N_{u,3}$	$N_{u,2}/N_{u,3}$	$N_{u,1}(\text{STCC})/N_{u,1}(\text{CFT})$	$N_{u,2}(\text{STCC})/N_{u,2}(\text{CFT})$
Average values	1.037	1.004	1.046	1.065
Dispersion coefficient	0.018	0.009	0.020	0.018

methods indicate that the ultimate load capacity of the circular STCC stub columns is slightly higher than that of the circular CFT stub columns with the same parameters.

4.2 Verification and comparisons

Table 2 Comparison of load bearing capacities from different methods

Specimen ID	Literature	$B \times t \times L$ (mm)	f_c (MPa)	f_s (MPa)	$N_{u,o}$ (kN)	$N_{u,c}$ (kN)				$N_{u,o}/N_{u,c}$			
						FE models	Elasto-plastic	Eq. (28)	Eq. (29)	FE models	Elasto-plastic	Eq. (28)	Eq. (29)
S30CL50B		165×2.82×562.5	48.3	363.3	1759	1848	1852	1851	1798	0.952	0.950	0.950	0.978
S30CL50C		165×2.82×571	38.2	363.3	1649	1654	1651	1649	1568	0.997	0.999	1.000	1.052
S20CL50C		190×1.94×659.5	38.2	256.4	1652	1578	1540	1539	1579	1.047	1.073	1.074	1.046
S16CL50B		190×1.52×658	48.3	306.1	1841	1953	1795	1794	1881	0.943	1.026	1.026	0.979
S12CL50C		190×1.13×657	38.2	185.7	1308	1332	1270	1269	1372	0.982	1.030	1.031	0.953
S10CL50C		190×0.86×657.5	38.2	210.7	1240	1306	1247	1247	1357	0.949	0.994	0.995	0.914
S30CL80C		190×2.82×581	56.4	363.3	2040	2120	2013	2012	1982	0.962	1.013	1.014	1.029
S20CL80C		190×1.94×655.5	56.4	256.4	2338	2416	2034	2034	2143	0.968	1.149	1.149	1.091
S16CL80A	O'shea and Bridge (2000)	190×1.52×658.5	80.2	306.1	2870	2951	2670	2670	2879	0.973	1.075	1.075	0.997
S12CL80C		190×1.13×661.5	56.4	185.7	1862	1968	1772	1773	1947	0.946	1.051	1.050	0.956
S10CL80B		190×0.86×657.5	74.7	210.7	2433	2437	2264	2263	2515	0.998	1.075	1.075	0.967
S10CL80C		190×0.86×664.5	56.4	210.7	1940	2033	1753	1753	1934	0.954	1.107	1.106	1.003
S30CL10C		165×2.82×571	56.4	363.3	2608	2714	2426	2425	2453	0.961	1.075	1.075	1.063
S20CL10C		190×1.94×656	77.1	256.4	3083	3129	2598	2597	2785	0.985	1.187	1.187	1.107
S16CL10C		190×1.52×658	77.1	306.1	2830	2914	2585	2585	2782	0.971	1.095	1.095	1.017
S12CL10C		190×1.13×662.5	77.1	185.7	2630	2697	2346	2346	2600	0.975	1.121	1.121	1.012
S12CL10A		190×1.13×661.5	108	185.7	3220	3315	3200	3201	3575	0.971	1.006	1.006	0.901
S10CL10C		190×0.86×664	77.1	210.7	2553	2613	2330	2330	2591	0.977	1.096	1.096	0.985
SC1-1		60×1.48×180	42.6	307	220	222	219	223	221	0.991	1.002	0.985	1.006
SC1-2		60×1.48×180	42.6	307	215	222	219	223	221	0.968	0.980	0.963	1.029
SC2-1		120×1.48×360	42.6	307	610	705	630	630	654	0.865	0.968	0.968	1.073
SC2-2		120×1.48×360	42.6	307	660	705	630	630	654	0.936	1.047	1.047	0.991
SC3-1	Han <i>et al.</i> (2005)	180×1.48×540	42.6	307	1311	1364	1218	1217	1296	0.961	1.077	1.077	0.988
SC3-2		180×1.48×540	42.6	307	1280	1364	1218	1217	1296	0.938	1.051	1.052	1.012
SC4-1		240×1.48×720	42.6	307	2300	2227	1985	1984	2084	1.033	1.159	1.159	0.933
SC4-2		240×1.48×720	42.6	307	2150	2227	1985	1984	2084	0.965	1.083	1.084	1.082
SZ3S6D	Yu <i>et al.</i> (2007)	165×2.76×500	77.2	350	2250	2255	2111	2110	2085	0.998	1.066	1.066	1.079
Average values										0.969	1.058	1.057	1.009
Dispersion coefficient										0.034	0.056	0.057	0.053

At present, limited formula is available to calculate the load bearing capacity of circular STCC stub columns as discussed in this study. Qing *et al.* (2010) proposed a formula to calculate the load bearing capacity of stub column and was used here to verify the modeling results and Eq. (28) proposed above. The formula proposed by Qing *et al.* (2010) is as below

$$N_u = (1.14 + 1.3\phi)f_c A_c \quad (29)$$

where $f_c = 0.67f_{cu}$.

To verify the practicability of the this formula, 27 groups of test data collected in O'shea and Bridge (2000), Han *et al.* (2005) and Yu *et al.* (2007) were compared with the calculated results from FE models, elasto-plastic analysis, Eqs. (28) and (29). The parameters of the selected test data are as follows: the diameter-to-wall thickness ratio

(D/t) ranged from 40 to 163, the concrete strengths (f_{cu}) ranged from 40 to 78 MPa, and the yield strength of steel (f_s) ranged from 300 to 359 MPa. The average ratio of the test data over the other results are shown in Table 2. It can be seen that the results calculated by Eq. (28) are in good agreement with the results obtained from FEA and the elasto-plastic methods. The FEA results are slightly higher than the theoretical results, and the results by elasto-plastic methods are close to the predicted results by Eq. (28), both of which are relatively safer.

5. Conclusions

This paper presents a combined numerical and theoretical study on the composite action between the steel and concrete of the STCC stub columns under axial compressive loadings with an elasto-plastic model and FE model in comparison with experimental results. Based on the studies and analysis, the following conclusions could be drawn:

- (1) Based on continuum mechanics, the elasto-plastic model for STCC stub columns was established and the analysis was realized by a FORTRAN program and a 3D FE model developed using the program ABAQUS. In general, the results obtained from the FE and the elasto-plastic methods are in good agreement with the experimental results.
- (2) The composite action between the steel and concrete of STCC and CFT stub columns with the same parameters were compared, and the results show that the circular STCC stub columns can achieve a better confinement effect. Moreover, it is found from the parametric study that when the friction coefficient between the steel tube and core concrete was defined as 0.4 to 0.6, the results of FE model have a good agreement with the elasto-plastic methods.
- (3) The influence of steel ratio on the confinement effect in STCC columns was identified by an extensive parametric study. When the steel ratio of the circular STCC column was between 0.5% and 2%, the confinement effect of steel tube to concrete was more obvious than circular CFT column with same steel ratio, which demonstrated the advantages of the circular STCC columns. Finally, the design formula of ultimate load capacity for the circular STCC stub column was also developed based on ultimate balance theory.

Acknowledgments

This research is jointly supported by the National Natural Science Foundation of China, Grant No. 51578548 and 51422814.

References

Aboutaha, R.S. and Machado, R. (1998), "Seismic resistance of steel confined reinforced concrete (SRC) columns", *Struct. Des. Tall. Spec.*, **7**(3), 251-260.

- Chang, X., Huang, C.K. and Chen, Y.J. (2009), "Mechanical performance of eccentrically loaded pre-stressing concrete filled circular steel tube columns by means of expansive cement", *Eng. Struct.*, **31**(11), 2588-2597.
- Cui, M.J. and Shao, Y.B. (2015), "Residual static strength of cracked concrete-filled circular steel tubular (CFCST) T-joint", *Steel Compos. Struct., Int. J.*, **18**(4), 1045-1062.
- Ding, F.X., Yu, Z.W. and Bai, Y. (2011a), "Elasto-plastic analysis of circular concrete-filled steel tube stub columns", *J. Constr. Steel Res.*, **67**(10), 1567-1577.
- Ding, F.X., Ying, X.Y., Yu, Z.W. and Ou, J.P. (2011b), "Mechanical performance of circular concrete-filled steel tube columns with lightweight aggregate concrete", *J. Shenzhen University. Science. Eng.*, **28**(3), 202-207. [In Chinese]
- Ding, F.X., Ying, X.Y., Zhou, L.C. and Yu, Z.W. (2011c), "Unified calculation method and its application in determining the uniaxial mechanical properties of concrete", *Front. Archit. Civil Eng. China*, **5**(3), 381-393.
- Ding, F.X., Fang, C.J. and Bai, Y. (2014), "Mechanical performance of stirrup-confined concrete-filled steel tubular stub columns under axial loading", *J. Constr. Steel Res.*, **98**(7), 149-157.
- Ding, F.X., Liu, J., Liu, X.M., Yu, Z.W. and Li, D.W. (2015), "Mechanical behavior of circular and square concrete filled steel tube stub columns under local compression", *Thin-Wall. Struct.*, **94**(9), 155-166.
- Ding, F.X., Li, Z., Cheng, S.S. and Yu, Z.W. (2016), "Composite action of hexagonal concrete-filled steel tubular stub columns under axial loading", *Thin-Wall. Struct.*, **107**(10), 502-513.
- Han, L.H., Yao, G.H., Chen, Z.P. and Yu, Q. (2005), "Experimental behavior of steel tube confined concrete (STCC) columns", *Steel Compos. Struct., Int. J.*, **5**(6), 459-484.
- Huang, Y.S., Long, Y.L. and Cai, J. (2008), "Ultimate strength of rectangular concrete-filled steel tubular (CFT) stub columns under axial compression", *Steel Compos. Struct., Int. J.*, **8**(2), 115-128.
- Huang, F.Y., Yu, X.M. and Chen, B.C. (2012), "The structural performance of axially loaded CFST columns under various loading conditions", *Steel Compos. Struct., Int. J.*, **13**(5), 451-471.
- Johansson, M. and Gylltoft, K. (2002), "Mechanical behavior of circular steel-concrete composite stub columns", *J. Struct. Eng.*, **128**(8), 1073-1081.
- Kim, W.W., Mun, J.H. and Yang, K.H. (2015), "Simplified model for the stress-strain relationship of confined concrete", *Steel Compos. Struct., Int. J.*, **31**(4), 79-86.
- Lee, S.H., Uy, B., Kim, S.H., Choi, Y.H. and Choi, S.M. (2011), "Behavior of high-strength circular concrete-filled steel tubular (CFST) column under eccentric loading", *J. Constr. Steel Res.*, **67**(1), 1-13.
- Liu, J.P., Zhang, S.M., Zhang, X.D. and Guo, L.H. (2009), "Behavior and strength of circular tube confined reinforced-concrete (CTRC) columns", *J. Constr. Steel Res.*, **65**(7), 1447-1458.
- O'shea, M. and Bridge, R.Q. (2000), "Design of circular thin-walled concrete filled steel tubes", *J. Struct. Eng.*, **126**(11), 1295-1303.
- Qing, Y., Tao, Z., Liu, W. and Chen, Z.B. (2010), "Analysis and calculations of steel tube confined concrete (STCC) stub columns", *J. Constr. Steel Res.*, **66**(1), 53-64.
- Ren, Q.X., Han, L.H., Lam, D. and Hou, C. (2014), "Experiments on special-shaped CFST stub columns under axial compression", *J. Constr. Steel Res.*, **98**(1), 123-133.
- Schneider, S.P. (1998), "Axially loaded concrete-filled steel tubes", *J. Struct. Eng.*, **124**(10), 1125-1138.
- Tomii, M., Sakino, K. and Xiao, Y. (1987), "Ultimate moment of reinforced concrete short columns confined in steel tube",

- Proc. of Pacific Conference on Earthquake Engineering.*,
Volume 2, pp. 11-22.
- Wang, Q.T. and Chang, X. (2013), "Analysis of concrete-filled steel tubular columns with "T" shaped cross section (CFTTS)", *Steel Compos. Struct., Int. J.*, **15**(1), 41-45.
- Yu, Z.W., Ding, F.X. and Cai, C.S. (2007), "Experimental behavior of circular concrete-filled steel tube stub columns", *J. Constr. Steel Res.*, **63**(2), 165-174.
- Zhou, X.H., Liu, J.P. and Zhang, S.M. (2009), "Behavior of circular tubed reinforced concrete stub columns under axial compression", *Eng. Mech.*, **26**(11), 53-59.
- Zhou, X.H. and Liu, J.P. (2010), *Performance and Design of Steel Tube Confined Members*, Science Press Ltd., Beijing, China.
[In Chinese]

DL